

Accelerated Articles

Anal. Chem. **1995**, *67*, 1–12

Capillary Electrophoresis Inductively Coupled Plasma Spectrometry for Rapid Elemental Speciation

John W. Olesik,^{*,†} Jeffery A. Kinzer,^{1,†} and Susan V. Olesik[‡]

Laboratory for Plasma Spectrochemistry, Laser Spectroscopy and Mass Spectrometry, Department of Geological Sciences, The Ohio State University, 1090 Carmack Road, Columbus, Ohio 43210, and Department of Chemistry, The Ohio State University, 120 West 18th Avenue, Columbus, Ohio 43210

Initial results using the combination of capillary electrophoresis (CE) and sensitive, element-selective, inductively coupled plasma (ICP) optical emission spectrometry (OES) and mass spectrometry (MS) for rapid elemental speciation are reported. An interface to produce a fine aerosol that is efficiently transported from the end of the electrophoresis capillary to the ICP with negligible liquid dead volume was developed. By using element-selective detection provided by ICP spectrometry, electrophoretic resolution could be traded off for rapid analysis times. CE-ICP spectrometry was used for elemental speciation of inorganic ions with different charge states, organometallic species, and metal–ligand complexes. CE-ICP spectrometry may also be useful to rapidly determine metal–ligand complex stability constants. Analysis times were generally less than 2 min. Detection limits for CE/ICP-OES were within a factor of 10 of those typically obtained using ICP-OES for elemental analysis (without speciation). Detection limits for CE/ICP-MS were generally a factor of 60 times higher than those typically obtained by using ICP-MS for elemental analysis (without speciation). However, the detection limits for CE/ICP-MS were as low as 0.06 ppb, which corresponds to 8 fg (90 amol) of Sr in the injected sample. Peak area and elution time reproducibility were typically better than 3% relative standard deviation for successive injections.

Metal speciation is important in a variety of environmental, biological, geological, and medical applications. Toxicity is often very species dependent. For example, arsenobetaine, commonly

found in shellfish, is nontoxic, while inorganic As is extremely toxic.¹ Cr(III) is an essential nutrient for humans. Cr(VI), sometimes used as an algicide, is toxic. While trace metals have long been known to be important for the health of plants, animals, and humans, the importance of speciation is just beginning to be unraveled. For example, the uptake of Cd by Swiss chard correlates with the Cd²⁺ activity, not the total Cd concentration.² The adsorption and transport of pollutants (such as free metal ions versus metal–ligand complexes^{3,4} or metal ions in different charge states⁵) from toxic waste sites and agricultural runoff are also highly species dependent. Many toxic waste sites contain organic solvents. Therefore, metal–ligand complexation in mixed-solvent systems is important. Removal of metal pollutants is also highly species dependent.

A variety of separation techniques have been used for quantitative elemental speciation analysis,^{6–8} including high-performance liquid chromatography (HPLC), ion chromatography (IC), supercritical fluid chromatography (SFC), and gas chromatography (GC). Element-selective detectors, including inductively coupled plasma (ICP) optical emission spectrometry (OES) and mass spectrometry (MS), microwave-induced plasma (MIP) OES and MS, direct current plasmas (DCP), graphite furnace atomic

- (1) Demesmay, C.; Olle, M.; Porthault, M. *Fresenius J. Anal. Chem.* **1994**, *348*, 205.
- (2) Bingham, F. T.; Strong, J. E.; Sposito, G. *Soil Sci.* **1983**, *135*, 160.
- (3) Doner, H. E. *Soil Sci. Soc. Am. J.* **1978**, *42*, 882.
- (4) Traina, S. J.; He, X. T.; Logan, T. J. *Agron. Abstr.* **1993**, 51.
- (5) Davis, J. A.; Kent, D. B.; Rea, B. A.; Maest, A. S.; Garabedian, S. P. In *Metals in Groundwater*; Allen, H. E., Purdeie, E. M., Brown, D. S., Eds.; Lewis: Chelsea, MI, 1993; pp 223–273.
- (6) Krull, I. S. *Trace Metal Analysis and Speciation*; Elsevier: Amsterdam, 1991.
- (7) Harrison, R. M.; Rapsomanikis, S. *Environmental Analysis Using Chromatography Interfaced with Atomic Spectroscopy*; John Wiley & Sons: New York, 1989.
- (8) Vela, N. P.; Olson, L. K.; Caruso, J. A. *Anal. Chem.* **1993**, *65*, 585A–597A.

^{*} Department of Geological Sciences.

[†] Department of Chemistry.

absorption (GFAA), and electrochemical techniques have been used in combination with separation techniques. Other detection methods, such as conductivity or photometric detection following postcolumn reaction, have also been used for elemental speciation.

In many cases, the fundamental and practical role of elemental speciation has been difficult to assess because of inadequate analytical techniques. Currently available techniques for quantitative elemental speciation often suffer from one or more of the following deficiencies: long analysis times, inadequate detection limits, amenable to a limited range of sample types, limited to measurement of a few species in one analysis, and insufficient selectivity.

The goal of the research described here is to develop a technique that will provide quantitative elemental speciation in less than 1 min with detection limits in the low ppb to sub-ppb range for a variety of sample types. If successful, quantitative elemental speciation could be accomplished in an amount of time similar to that now required for elemental analysis alone by inductively coupled plasma spectrometry. We seek to quantitatively determine the concentrations of free ions with different charge states, metal–ligand complexes (both weak and stable), and organometallic species.

In order to pursue the goal of rapid, quantitative, sensitive elemental speciation, the high selectivity, speed, and sensitivity of inductively coupled plasma spectrometry were combined with the high separation efficiency, speed, and chemical simplicity of capillary electrophoresis (CE). The high selectivity of ICP spectrometry allows resolution of the chemical separation to be traded off for rapid analysis times. There is no need to electrophoretically separate species containing different elements from each other. The electrophoresis is only required to separate different species of the same element such as Cr(III) from Cr(VI), Fe(II) from ferrocene, and Cu^{2+} from $\text{Cu}(\text{EDTA})^{2-}$.

While capillary electrophoresis has been used mainly to separate large, organic molecules,^{9–11} it can also be effectively used to separate different metal ions.^{12–17} Capillary electrophoresis, sometimes called capillary ion analysis,^{18–20} has been used for elemental analysis with nonselective indirect UV absorbance or indirect fluorescence detection.^{14–20} The separation of free metal ions is related to their equivalent ionic conductances. Monovalent metal ions such as Na^+ , K^+ , and Cs^+ are easily separated because their equivalent ionic conductances (50 , 73 , and $78 \times 10^{-4} \text{ m}^2 \Omega^{-1} \text{ mol L}^{-1}$ at 25°C , respectively²¹) vary widely.

Many divalent metal ions, such as Cu^{2+} , Fe^{2+} , and Mg^{2+} , are difficult to separate because their equivalent ionic conductances (107.2×10^{-4} , 108×10^{-4} , and $106 \times 10^{-4} \text{ m}^2 \Omega^{-1} \text{ mol L}^{-1}$ at 25°C , respectively) are similar. Many trivalent metal ions, such as

Fe^{3+} and Cr^{3+} , are difficult to separate because their equivalent ionic conductances (156×10^{-4} and $154 \times 10^{-4} \text{ m}^2 \Omega^{-1} \text{ mol L}^{-1}$, respectively) are similar. Mixtures of ions with similar ionic mobilities, such as lanthanides, cannot be separated by capillary electrophoresis unless an additional separation mechanism is used.^{18,19} These ions can be separated by capillary electrophoresis if a complexing electrolyte that has different stoichiometry for different elements or is weakly complexing to different degrees with each element is used.^{14–16,22–25} Detection schemes including indirect UV absorbance detection,²⁶ direct UV absorbance detection of complexed metal ions,²⁷ indirect fluorescence,²⁸ direct fluorescence of complexed metal ions,²⁹ holographic refractive index,³⁰ conductivity,³¹ amperometry,³² and ion spray mass spectrometry^{33,34} have been used with capillary electrophoresis for metal ion analysis.

Unlike previous reports on capillary electrophoresis for metal ion analysis (with few exceptions^{35,36}), we seek to preserve and quantitatively measure the different species in which each element exists in the sample, rather than measuring total element concentrations. The use of a complexing electrolyte to enhance the separability of different element ions, as has been commonly done, could lead to a loss of speciation information in the original sample (if the fraction of free versus bound ions was of interest, for example). Therefore, noncomplexing electrolytes are needed.

By using an element-selective detector, different elements that exist as ions of the same charge (such as Fe^{2+} and Sr^{2+}) do not need to be electrophoretically separated. Only ions, complexes, or molecules containing the same element need to be separated. The equivalent ionic conductances of an element in its different charge states, such as Fe^{2+} and Fe^{3+} (108×10^{-4} and $156 \times 10^{-4} \text{ m}^2 \Omega^{-1} \text{ mol L}^{-1}$, respectively) or Cr^{3+} and $\text{Cr}_2\text{O}_7^{2-}$, are widely different. Therefore, these species should be relatively easy to separate in a short time.

Electrophoretic resolution could be traded off for analysis speed since ions with similar mobilities (different elements that exist as ions of the same charge) do not need to be electrophoretically separated. Separation times of 5–30 min are typically required for capillary electrophoresis separation of metal ions using nonselective detection. Analysis times of 1 min or less should be attainable by taking advantage of an element-selective detector. The combination of capillary electrophoresis (with its high separation efficiency) and inductively coupled plasma optical emission or mass spectrometry (with its high selectivity and low

(9) Jorgenson, J. W.; Lukacs, K. D. *Science* **1984**, *222*, 266.

(10) Kuhr, W. G.; Monnig, C. A. *Anal. Chem.* **1992**, *64*, 389R.

(11) Righetti, P. G. *J. Chromatogr. Libr.* **1992**, *51*, A481.

(12) Hjertén, S. *Chromatogr. Rev.* **1967**, *9*, 122.

(13) Tsuda, T.; Nomura, K.; Nakagawa, G. *J. Chromatogr.* **1983**, *264*, 385.

(14) Chen, M.; Cassidy, R. M. *J. Chromatogr.* **1993**, *640*, 425.

(15) Timerbaev, A. R.; Buchberger, W.; Semenova, O. P.; Bonn, G. K. *J. Chromatogr.* **1993**, *630*, 379.

(16) Rivello, J. M.; Harrold, M. P. *J. Chromatogr.* **1993**, *652*, 385.

(17) Fritz, J. S.; Youchun, S. *J. Chromatogr.* **1993**, *640*, 473.

(18) Jandik, P.; Jones, W. R.; Weston, A.; Brown, P. R. *LC-GC* **1991**, *9*, 634.

(19) Weston, A.; Brown, P. R.; Heckenberg, A. L.; Jandik, P.; Jones, W. R. *J. Chromatogr.* **1992**, *602*, 249.

(20) Jones, W. R.; Jandik, P. *J. Chromatogr.* **1992**, *608*, 385.

(21) Vanýsek, P. In *CRC Handbook of Chemistry and Physics*, 68th ed.; Weast, R. C., Astle, M. J., Beyer, W. H., Eds.; CRC Press: Boca Raton, FL, 1987; pp D167–D169.

(22) Shi, Y.; Fritz, J. S. *J. Chromatogr.* **1993**, *640*, 473.

(23) Foret, F.; Fanali, S.; Nardi, A.; Boček, P. *Electrophoresis* **1990**, *11*, 780.

(24) Lin, T.-I.; Lee, Y.-H.; Chen, Y.-C. *J. Chromatogr. A* **1993**, *654*, 167–176.

(25) Lee, Y.-H.; Lin, T.-I. *J. Chromatogr. A* **1994**, *675*, 227–236.

(26) Weston, A.; Brown, P. R.; Jandik, P.; Jones, W. J.; Heckenberg, A. L. *J. Chromatogr.* **1992**, *593*, 289–295.

(27) Timerbaev, A.; Semenova, O.; Bonn, G. *Chromatographia* **1993**, *37*, 497–500.

(28) Gross, L.; Yeung, E. *Anal. Chem.* **1990**, *62*, 247.

(29) Swaile, D. F.; Sepeniak, M. J. *Anal. Chem.* **1991**, *63*, 179–184.

(30) Krattiger, B.; Bruin, G. J. M.; Bruno, A. E. *Anal. Chem.* **1994**, *66*, 1–8.

(31) Huang, X.; Pang, T.-K. J.; Gordon, M. J.; Zare, R. N. *Anal. Chem.* **1987**, *59*, 2747–2749.

(32) Lu, W.; Cassidy, R. M. *Anal. Chem.* **1993**, *65*, 1649–1653.

(33) Huggins, T. G.; Henion, J. D. *Electrophoresis* **1993**, *14*, 531–539.

(34) Corr, J.; Covey, T. C.; Anaceito, J. F. *Proceedings of the 42nd ASMS Conference on Mass Spectrometry and Allied Topics*, Chicago, IL, May 29–June 3, 1994; paper 340.

(35) Morin, P.; Amran, M. B.; Favier, S.; Heimburger, R.; Leroy, M. *Fresenius J. Anal. Chem.* **1992**, *342*, 357–362.

(36) Medina, I.; Rubi, E.; Mejuto, M. C.; Cela, R. *Talanta* **1993**, *40*, 1631–1636.

concentration detection limits) has the potential to provide rapid, sensitive metal speciation.

Many elements have limits of detection less than 10 parts per trillion in ICP-MS when a conventional nebulizer/spray chamber sample introduction system is used. Assuming an analyte transport efficiency from the nebulizer into the plasma of 1.5%, a liquid uptake rate of 1.0 mL/min and a detection limit of 0.010 ppb, the detection limit in terms of analyte entering the plasma per second is ~ 2.5 fg/s. Similar absolute detection limits could be expected for CE/ICP-MS if the analyte was transported into the plasma with 100% efficiency, if the signal per picogram of sample entering the plasma per second was maintained, and if there were no other losses of analyte.

One key to successfully coupling capillary electrophoresis and ICP spectrometry is the interface. The interface must minimize electrophoretic band broadening and it must effectively deliver sample aerosol into the plasma (with as high an efficiency as possible in a form that is easily vaporized, atomized and ionized, or excited).

This paper describes initial CE-ICP optical emission and mass spectrometry results for rapid elemental speciation. A simple, low dead volume interface between the electrophoresis capillary and the ICP is described. The basic principles and viability of CE-ICP spectrometry are shown. The role of the electrophoresis electrolyte is discussed. The efficiency of analyte transport from the electrophoresis capillary and signal production in the ICP is assessed.

EXPERIMENTAL SECTION

Capillary Electrophoresis. Fused silica capillaries (Polymicro Technologies) with an inner diameter of $97\ \mu\text{m}$ and an outer diameter of $130\ \mu\text{m}$ were used. The capillary was 40–50 cm long. A high-voltage dc power supply (Hipotronics Model 10B) provided a voltage of up to 10 kV between the ends of the capillary. The inlet end of the capillary was held at a positive potential while the outlet end was grounded. A nichrome ribbon was used as the electrode in the supply electrolyte reservoir. Contamination due to Ni and Cr from the nichrome wire was observed if the electrolyte solution in the supply reservoir was not replaced often. Electrophoretic currents were measured using a Fluke 8020B multimeter in the ammeter mode placed in the circuit between the electrical connection to outlet end of the capillary and the ground of the high-voltage power supply. Typical electrophoretic currents through the capillary were 5–10 μA . The capillary volume was $\sim 4.3\ \mu\text{L}$.

Chemical Reagents. The following electrolytes were used (in separate experiments): sodium acetate (99.3% pure, Baker), sodium chloride (99.989% pure, Fisher), and calcium chloride (99.9%, Fisher). The following solids were used for analyte species: $\text{CaCl}_2 \cdot 2\text{H}_2\text{O}$ (99.9% pure, Fisher), $\text{SrCl}_2 \cdot 6\text{H}_2\text{O}$ (99% pure, Aldrich), SrCO_3 (98% pure, Aldrich), $\text{K}_2\text{Cr}_2\text{O}_7$ (99.9% pure, Mallinckrodt), $\text{FeCl}_2 \cdot 4\text{H}_2\text{O}$ (99.7% pure, Baker), $\text{FeCl}_3 \cdot 6\text{H}_2\text{O}$ (97.0–102.0% assay, EM Science), $\text{SnCl}_4 \cdot 5\text{H}_2\text{O}$ (purified grade, Fisher), $\text{SnCl}_2 \cdot 5\text{H}_2\text{O}$ (98.1% pure, Fisher), As_2O_3 (99% pure, Aldrich), $\text{C}_2\text{H}_5\text{AsNaO}_2 \cdot 2\text{H}_2\text{O}$ (analytical grade, Kodak), $\text{CuSO}_4 \cdot 2\text{H}_2\text{O}$ (96.4% pure, Fisher) and $\text{Na}_2\text{H}_2\text{EDTA} \cdot 2\text{H}_2\text{O}$ (99.0%, GFS Chemicals).

Nebulizer. Meinhard type TR-30-A3 and SB-30-A3 nebulizers (J. E. Meinhard and Associates) were used. The Ar gas flow rate through the nebulizer was controlled with a mass flow controller (MKS Model 1159B with Model 246 readout).

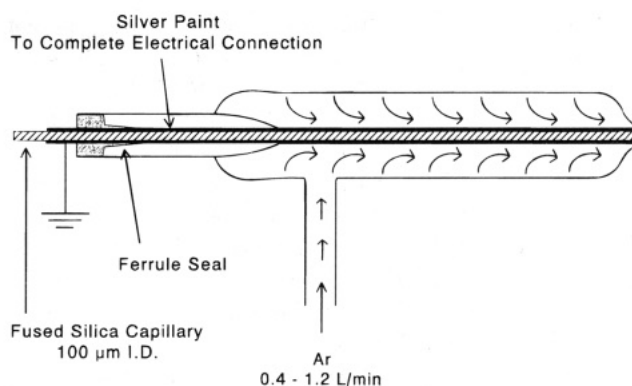


Figure 1. Diagram of interface between the electrophoresis capillary and the concentric, pneumatic nebulizer.

Connection between the Electrophoresis Capillary and the Nebulizer. The nebulizer–capillary connection is shown in Figure 1. The outside 4–5 cm of the capillary was coated with silver paint (GC Chemicals), which served two purposes. First, the conducting silver paint provided a connection between the solution at the tip of the capillary and ground. Second, the thickness of the silver paint was controlled so that the coated capillary outer diameter fit tightly into the center tube of the concentric, pneumatic nebulizer. Silver paint was applied with a fine brush. Thickness was manipulated using very fine emery paper to sand a smooth coating which fit tightly into the nebulizer. The end of the electrophoresis capillary was placed within 0.5 mm of the tip of two tubes making up the concentric, pneumatic nebulizer. Under some conditions, particularly if a ligand is present at high concentrations that complexes strongly with Ag, contamination of the capillary effluent with Ag can occur.

Liquid Flow Rates. The electroosmotic flow through the capillary (0.04 M sodium citrate electrolyte, 10 kV) was determined to be $0.051 \pm 0.014\ \mu\text{L}/\text{min}$ by measuring the mass of liquid deposited in a volumetric flask at 5, 10, 15, 20, and 60 min intervals. There was a second contribution to the liquid flow through the capillary. A slight vacuum is formed due to the fast moving gas exiting the nebulizer, which resulted in a natural aspiration rate of $\sim 2.0\ \mu\text{L}/\text{min}$ at a nebulizer gas flow rate of 1.0 L/min.

Spray Chambers. The purpose of a spray chamber in ICP spectrometry is to prevent large droplets from entering the plasma and to limit the total aerosol transport rate (to typically less than $20\ \mu\text{L}$ of aqueous aerosol/min). A Scott-type spray chamber³⁷ or a conical spray chamber with impact bead are commonly used to prevent excessive aerosol solvent loading of the ICP. Because the total liquid flow rate through the capillary was so small, an open, conical, locally constructed spray chamber (similar to the ARL type but without the impact bead; similar to Rocky Mountain Scientific Glass Blowing Model SAR-S04) was used to increase the analyte transport efficiency compared to a Scott-type double-pass spray chamber or a spray chamber with an impact bead.

Aerosol Size Measurements. An Aerometrics phase doppler particle analyzer (Model XMT-1100 one-dimensional transmitter, RCV-2100 receiver with three photomultiplier tubes, PDP-3100 phase/Doppler processor, and MCS-7100 motor controller) was used to measure primary aerosol drop size distribution^{38,39}

(37) Scott, R. H.; Fassel, V. A.; Knisely, R. N.; Nixon, D. E. *Anal. Chem.* **1974**, *46*, 75–80.

(38) Bachalo, W. D.; Houser, M. J. *Opt. Eng.* **1984**, *23*, 583.

produced by the nebulizer (with inserted capillary).

Inductively Coupled Plasma Optical Emission Spectrometer. An ARL 34000 direct-reading ICP optical emission spectrometer was used. A standard ARL ICP torch was used with an outer gas flow rate of 15 L/min and an intermediate gas flow rate of 1 L/min. A power of 1.1 kW was used. Current from each photomultiplier tube observing a line of interest was converted to voltage by a Keithley 427 current amplifier. The voltages were digitized at a rate of 5 Hz by a 12-bit Tecmar Lab Master board in a Zeos 386SX or Gateway DX486/33 computer under control of a laboratory-written ASYST program.

Inductively Coupled Plasma Mass Spectrometer. A Perkin-Elmer Sciex ELAN 5000 ICP mass spectrometer was used. A standard torch for this instrument was used with an outer Ar gas flow rate of 15 L/min and an intermediate gas flow rate of 0.8 L/min. The applied power was 1.0 kW. The ion optics settings were standard settings recommended when a conventional nebulizer/spray chamber is used with a liquid sample uptake rate of 1.0 mL/min. Signals from six elements were monitored in a peak-hopping mode. A dwell time of 100 ms was used. The electropherogram (signals from all six elements) was acquired at a rate of 1.4 Hz.

Sample Injection. A volume of 0.14 or 0.080 μL of sample (depending on the capillary length; experimentally measured as discussed below) was hydrodynamically injected into the electrophoresis capillary while the nebulizer gas was off. The sample was raised to a height 11 in. above the outlet end of the capillary for 15 s in all cases. The inlet end of the capillary was then placed in the electrolyte reservoir, and the nebulizer gas was turned on.

Data Processing and Modeling. PeakFit (Jandel Scientific) was used to determine peak areas and peak widths. Unless otherwise noted, peak widths were the full width at half-maximum. The peak width was calculated by using PeakFit with either a Gaussian or exponentially modified Gaussian peak shape assumed. MINTEQA2 (U.S. Environmental Protection Agency Center for Exposure Assessment Modelling, Athens, GA, Equilibrium Metal Speciation Model 3.11, December 1991) was used to predict equilibrium concentrations of free metal ions and metal-ligand complexes.

RESULTS AND DISCUSSION

Capillary electrophoresis separates on the basis of mobility in response to a voltage gradient along the capillary.⁴⁰ The mobility of a species is related to the charge on the species and its size. The outlet end of the capillary was at a high negative potential relative to the inlet end. Because there was a bulk flow of liquid from the inlet to the outlet of the capillary (due to the combination of electroosmotic flow and nebulizer suction-driven flow) that moved at a faster rate than the migration of negative ions toward the inlet, negative, neutral, and positive ions all eluted from the capillary. The most highly positive ions eluted first; the most negatively charged ions eluted last.

The basic concepts of CE-ICP spectrometry are illustrated by the electropherograms shown in Figures 2 and 3. Optical emission produced in the ICP was detected from Fe at 259.9 nm and from Cr at 267.7 nm simultaneously by a direct-reading spectrometer (Figure 2). Cr(III), which exists as the neutral

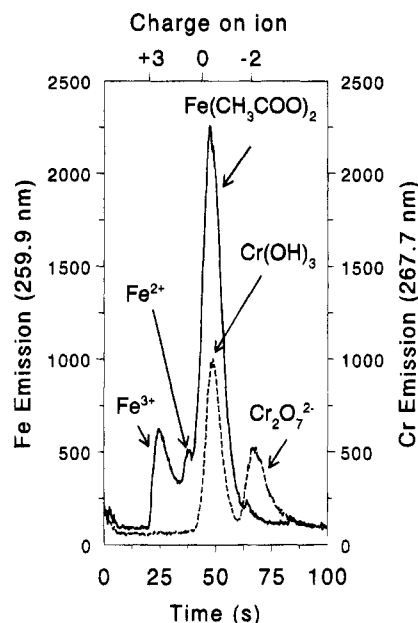


Figure 2. Electropherogram of a series of chromium (total chromium concentration was 100 $\mu\text{g/mL}$) and iron (total iron concentration was 100 $\mu\text{g/mL}$) compounds detected by ICP-OES. The electrolyte was 0.04 M sodium acetate, pH was ~ 8.2 . A voltage of 10 kV was applied.

molecule $\text{Cr}(\text{OH})_3$ in water at basic pH, was well separated from Cr(VI), which exists as $\text{Cr}_2\text{O}_7^{2-}$. The $\text{Cr}(\text{OH})_3$ eluted first because it is a neutral compound, while the $\text{Cr}_2\text{O}_7^{2-}$ is negatively charged. Fe(III), as Fe^{3+} , and $\text{Fe}(\text{CH}_3\text{COO})_2$ are separated although not baseline resolved. Fe(II), present in small concentration as Fe^{2+} , appears as a small peak on the shoulder of the peak due to $\text{Fe}(\text{CH}_3\text{COO})_2$. Fe^{3+} , which is the most highly positively charged species, eluted before Fe^{2+} , which eluted before neutral $\text{Fe}(\text{CH}_3\text{COO})_2$. $\text{Fe}(\text{CH}_3\text{COO})_2$ and $\text{Cr}(\text{OH})_3$ coelute. However, the Fe and Cr are selectively detected by the ICP spectrometer so that electrophoretic separation of the $\text{Fe}(\text{CH}_3\text{COO})_2$ and $\text{Cr}(\text{OH})_3$ is not necessary for quantitative analysis. The analysis was completed in less than 100 s.

Figure 3 shows the ICP-MS-detected capillary electropherogram. Most elements exist mainly as singly charged ions in the ICP, regardless of their form in the original sample. Signals were detected at mass to charge ratios of 52 (Cr^+), 75 (As^+), 88 (Sr^+), and 120 (Sn^+) due to Cr(III) mainly as $\text{Cr}(\text{OH})_2^+$ at the pH of this solution, and Cr(VI) as $\text{Cr}_2\text{O}_7^{2-}$, As(III) as HAsO_2 , As(V) as H_2AsO_4^- , Sn(IV) as Sn^{4+} , and Sr(II) as Sr^{2+} . Each species was present in the original sample present at a concentration of 1 ppm of the metal. The high signal to noise ratio is consistent with detection limits that are less than 1 part per billion (ppb) for the Sr and Sn species and ~ 1 ppb for the As and Cr species, as discussed further below. The peaks for the Sr^{2+} and $\text{Cr}(\text{OH})_2^+$ overlap significantly. There is a slight difference in elution times (49.3 s for Sr^{2+} and 51.2 s for $\text{Cr}(\text{OH})_2^+$), probably due to their size difference. It may be possible to electrophoretically separate these two species by using a longer capillary with the same voltage gradient per centimeter of capillary, but elution times, and therefore the total analysis time, would increase. Alternatively, a higher voltage could be applied to the same length capillary, as long as Joule heating did not have a deleterious effect on the resolution. Because the ICP-MS is an element-selective detector, there is no need to electrophoretically separate the Sr^{2+} from the

(39) Clifford, R. H.; Ishii, I.; Montaser, A.; Meyer, G. A. *Anal. Chem.* **1990**, *62*, 390.

(40) Oda, R. P.; Landers, J. P. In *Handbook of Capillary Electrophoresis*; Landers, J. P., Ed.; CRC Press: Boca Raton, FL, 1994; pp 10–41.

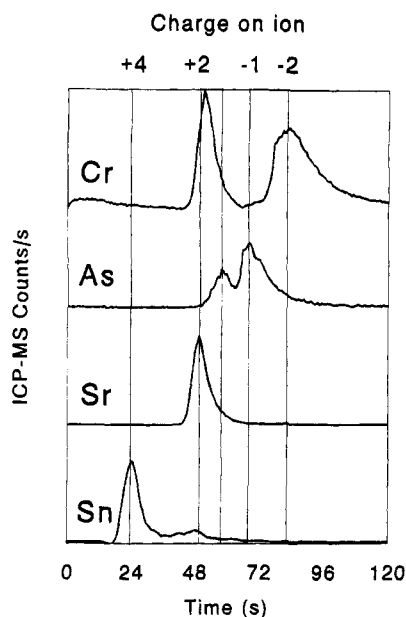


Figure 3. Electropherogram of a series of tin (Sn^{4+} and a small amount of Sn^{2+}), strontium (Sr^{2+}), arsenic (As(III) as HAsO_2 , As(V) as H_2AsO_4^-), and chromium (Cr(III) as CrOH^{2+} and Cr(VI) as $\text{Cr}_2\text{O}_7^{2-}$). Each species (with the exception of Sn^{2+}) was present at a concentration of 1 ppm. A voltage of 10 kV was applied. The electrolyte was 0.06 M calcium chloride; pH was ~ 6.7 . The electropherograms are offset vertically for illustration. The maximum and minimum ICP-MS count rates (in counts per second) observed at the mass corresponding to the major isotope of each analyte were as follows: Cr, 107 000 and 5100; As, 5600 and 10; Sn, 30 400 and 200; Sr, 76 000 and 200.

$\text{Cr}(\text{OH})^{2+}$, so electrophoretic resolution can be sacrificed in order to shorten analysis times.

Interface. The interface between the end of the electrophoresis capillary and the inductively coupled plasma is key to the success of the CE-ICP spectrometry technique. Unlike UV-visible or fluorescence detection, which can be performed on-column, the electrophoresis effluent must be physically transported from the capillary to the plasma. The capillary electrophoresis liquid flow rate is typically less than $2 \mu\text{L}/\text{min}$. Therefore, the dead volume must be minimal. Furthermore, aerosol must be efficiently produced and transported into the plasma. Typical aerosol transport rates for ICP spectrometry are on the order of $5\text{--}20 \mu\text{L}/\text{min}$. However, sample uptake rates are typically $\sim 1 \text{ mL}/\text{min}$, so less than 2% of the sample aerosol reaches the plasma. Therefore, aerosol produced from the effluent of the electrophoresis capillary must be efficiently transported into the plasma to prevent substantial loss in sensitivity (signal/concentration of analyte in sample). Finally, an electrical connection must be made between the electrolyte in the capillary and the electrophoresis power supply.

The CE-pneumatic nebulizer interface, which generated an aerosol from the end of the electrophoresis capillary, as described in the Experimental Section, produced a primary aerosol with a Sauter mean diameter of $4.2 \mu\text{m}$ at a nebulizer flow rate of $1.0 \text{ L}/\text{min}$. The value of $4.2 \mu\text{m}$ is similar to the tertiary aerosol Sauter mean diameters typically observed⁴¹ when a nebulizer and double-pass spray chamber are used with a sample uptake rate of $1.0 \text{ mL}/\text{min}$. The combination of a fine primary aerosol and a small

total liquid flow rate obviates the need to use an inefficient spray chamber to remove large aerosol droplets or to reduce the total aerosol loading.

Capillary electrophoresis has been combined with mass spectrometry using an electrospray ionization (ESI) interface.⁴² Similar to CE-ICP spectrometry, the sample must be physically transported to the mass spectrometer. The most popular interface for CE/ESI-MS uses a liquid sheath flow design,⁴³ although other designs have also been used.⁴² The liquid sheath flow design produces some dilution of the sample although sensitivity losses are not as large as a simple ratio of the electroosmotic to total electroosmotic and sheath flow rates. It is likely that a liquid sheath flow design would also be effective for CE/ICP-MS although primary aerosol drop sizes may increase with an increase in total liquid to nebulizer gas ratio. Some loss of sensitivity may result, particularly in ICP-OES, if solvent loading increases significantly or if the aerosol number density in the spray chamber increases, leading to more extensive drop coagulation and loss.

Band Broadening. Peak widths depend on the sample injection plug length, the amount of sample focusing (stacking), sources of band broadening while the analyte is in the capillary, and dead volume between the end of the capillary and the detector. Band broadening in the electrophoresis capillary can originate from analyte diffusion in the capillary, reduced local voltage gradients near the analyte if the analyte conductivity is similar to or greater than that of the electrophoresis electrolyte, a nonoptimum flow profile in the capillary, liquid dead volume, and slow aerosol transport from the nebulizer to the plasma (due to gas mixing or aerosol deposition in the spray chamber).

Based on the injected volume ($0.14 \mu\text{L}$) and the measured liquid flow rate through the capillary ($2.0 \mu\text{L}/\text{min}$), the expected peak width can be estimated. In 4.2 s, $0.14 \mu\text{L}$ of solution will exit the capillary. Therefore, if no dispersion or focusing of the analyte occurred in the capillary and there was no postcapillary band broadening, the peak would be $\sim 4 \text{ s}$ wide. Typically, the experimental peak widths were 8–15 s width (full width at half-maximum) although peak widths as narrow as 2 s were observed in some cases.

When the conductivity of the sample is lower than that of the electrophoresis electrolyte, the voltage gradient (V/cm) is higher in the sample plug than in the electrolyte. As a result, charged ions migrate faster in the sample plug, which produces focusing or "stacking" of the sample ions into a smaller volume than the injection volume.⁴⁴ This leads to band narrowing, as shown in Figure 4. When no voltage is applied, the zone is pulled through the capillary due to the suction produced by the nebulizer. When a high voltage is applied, solvent flow through the capillary is due to a combination of the nebulizer suction and electroosmotic flow. The peak width is narrower when the high voltage is applied than when no voltage is applied due to two factors: electrostatic focusing and less time spent in the capillary when voltage is applied (and, therefore, less diffusion). Thus, it is desirable to use an electrolyte that has a higher conductivity than the sample solution. This is discussed further below.

(42) Smith, R. D.; Wahl, J. H.; Goodlett, D. R.; Hofstadler, S. A. *Anal. Chem.* **1993**, *65*, 574A–584A.

(43) Smith, R. D.; Barinaga, C. J.; Udeseth, H. R. *Anal. Chem.* **1988**, *60*, 1948–1952.

(44) Albin, M.; Grossman, P. D.; Moring, S. E. *Anal. Chem.* **1993**, *65*, 489A–496A.

(41) Browner, R. F.; Canals, A.; Hernandis, V. *Spectrochim. Acta* **1992**, *47B*, 659–673.

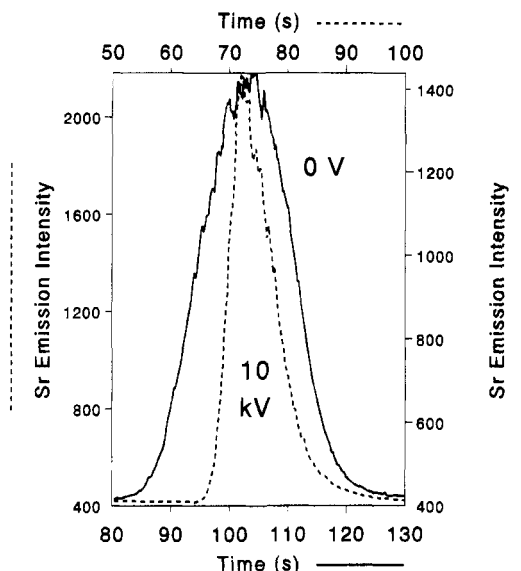


Figure 4. Comparison of peak shapes (Sr^{2+} injected into 0.06 M calcium chloride electrolyte, pH ~ 8) when the applied voltage is 0 or 10 kV. The zone is pulled through the capillary due to suction produced by the nebulizer when no voltage is applied, with an increase in solvent flow rate due to electroosmotic flow when 10 kV is applied. Bottom x axis and right y axis are for 0 kV case; top x axis and left y axis are for the 10 kV case.

Electroosmotic flow produces a flow with virtually constant velocity as a function of radial position within the capillary.⁴⁵ Forced flow, induced by suction created at the tip of the nebulizer, produces a parabolic-shaped velocity profile as a function of radial position in the capillary, which likely degrades resolution. The liquid flow rate through the capillary is ~ 40 times larger than the electroosmotic flow. Band broadening due to the laminar flow profile was estimated to be ~ 3 s from a calculation of the theoretical variance. The forced solvent flow rate due to the nebulizer suction could be reduced by using an electrophoresis capillary with a smaller inner diameter, at the expense of poorer concentration-based detection limits.

If the conductivity of the electrophoresis electrolyte is too high, Joule heating will be large enough to increase the temperature of the electrophoresis electrolyte and to produce radial temperature gradients in the capillary.^{46–48} As the temperature increases, the density and viscosity of the solution will decrease, which leads to increased diffusion rates and degradation of resolution. If thermal gradients are produced in the capillary, convection currents will produce mixing. The effect of Joule heating can be reduced by using an electrophoresis capillary with a smaller diameter, with some degradation of concentration-based detection limits, or by actively cooling the capillary.

If the conductivity of the electrophoresis electrolyte is too low compared to the conductivity of the sample, the voltage gradient in the injected sampled plug and near the analyte zone(s) in the capillary will always be smaller than the voltage gradient in the electrolyte solution. As a result, electrophoretic peaks will become distorted, similar to that observed when chromatographic columns

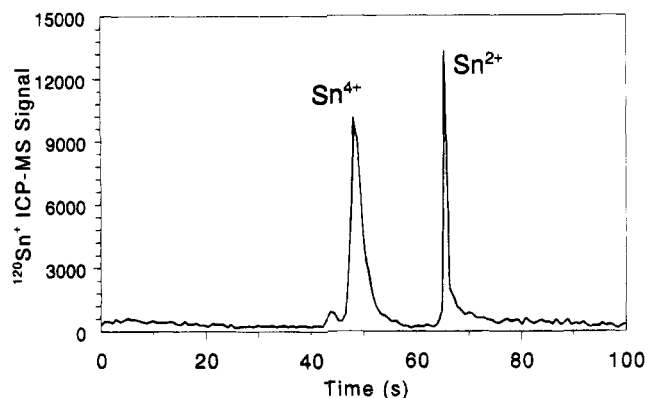


Figure 5. CE/ICP-MS electropherogram of 1 ppm Sn^{4+} and 1 ppm Sn^{2+} : 0.04 M NaCl electrolyte, pH ~ 7 , and 10 kV applied voltage.

are overloaded. It is recommended that the concentration of the electrophoresis electrolyte be at least a 1000 times the concentration of the sample.⁴⁵

The upper limit on the conductivity of the electrophoresis electrolyte due to Joule heating and the lower limit on the ratio of the conductivity of the electrolyte to the conductivity of the sample will limit the highest concentration of analytes that can be effectively separated in samples.

The optimum resolution and peak shape should be obtained when the mobility of the analyte is similar to the mobility of the similarly charged ion in the electrolyte.^{18,49,50} If the mobility of the analyte is dramatically different from that of the electrolyte ion, unstable boundaries and mixing can result in fronting or tailing of peaks, depending on the relative mobilities.

The electrophoresis eluent is converted into an aerosol at the end of the electrophoresis capillary with no dilution due to a make-up buffer solution, as is commonly used for CE-electrospray MS, or postcapillary connection to a nebulizer. Therefore, there should be no band broadening due to the interface in the liquid phase.

Another potential source of band broadening is the spray chamber. The volume of the spray chamber was ~ 60 mL. At a gas flow rate of 1 L/min, the gas in the spray chamber should be replaced in 3.6 s, assuming no mixing occurs. However, there will be some mixing, so the aerosol in the spray chamber will require more than 3.6 s to be swept into the plasma. Typical washout times for spray chambers in ICP spectrometry (for the signal to fall to 1% of its original magnitude), when the liquid uptake rate is 1.0 mL/min, are 10–30 s.

The ICP-MS-detected electropherogram of Sn(II) and Sn(IV) is shown in Figure 5. The full width at half-maximum of the Sn(II) peak is less than 2 s. This suggests that the spray chamber does not contribute greatly to band broadening measured as the full width at half-maximum. However, the spray chamber may contribute to the tailing observed on this peak.

Choice of Electrolyte. As discussed above, the conductivity of the electrophoresis electrolyte must be properly chosen. The relative conductivities of different electrolytes can be estimated from their conductivities⁵¹ (defined as the concentration of NaCl which has the same electrical conductance as the substance in

(45) Wallingford, R. A.; Ewing, A. G. In *Advances in Chromatography: Biotechnological Applications and Methods*; Giddings, J. C., Grushka, E., Brown, P. R., Eds.; Marcel Dekker Press: New York, 1989; pp 1–76.

(46) Gas, B. J. *Chromatogr.* **1993**, *644*, 161.

(47) Bello, M. S.; Righetti, P. G. *J. Chromatogr.* **1992**, *606*, 95.

(48) Knox, J. H. *Chromatographia* **1988**, *26*, 329.

(49) Mikkers, F. E. P.; Everaerts, F. M.; Verheggen, T. P. M. *J. Chromatogr.* **1979**, *169*, 18.

(50) Hjerten, S. *Electrophoresis* **1990**, *11*, 665.

(51) Wolf, A. V.; Morden, G. B.; Phoebe, P. G. In *CRC Handbook of Chemistry and Physics*, 68th ed.; Weast, R. C., Astle, M. J., Beyer, W. H., Eds.; CRC Press: Boca Raton, FL, 1987; pp D219–D269.

Table 1. Effect of Electrolyte, Applied Voltage, and Charge on Cation on ICP-MS Sensitivity due to Trapping of Analyte Ions in the Stern Layer^a

electrolyte	applied voltage (kV)	peak area (voltage applied)/ peak area (no voltage)			
		0.02 ppm Co ²⁺	0.2 ppm Co ²⁺	2 ppm Co ²⁺	20 ppm Co ²⁺
NaCl	4	0.27	0.50	0.60	0.66
CaCl ₂	4	0.92	1.06	0.98	0.99
NaCl	10	0.22	0.37	0.32	0.47
CaCl ₂	10	0.40	0.87	0.72	0.82

electrolyte	applied voltage (kV)	peak area (voltage applied)/ peak area (no voltage)			
		0.02 ppm Li ⁺	0.2 ppm Li ⁺	2 ppm Li ⁺	20 ppm Li ⁺
NaCl	4	0.77	0.81	0.90	0.91
CaCl ₂	4	0.98	0.96	1.02	0.98
NaCl	10	0.64	0.74	0.88	0.89
CaCl ₂	10	0.51	0.69	0.61	0.86

^a Concentration of NaCl was 0.04 M; concentration of CaCl₂ was 0.023 M so that the conductivity was the same for both electrolytes. Relative standard deviations for these data were typically 5–8%.

question). Using conductivity data, the following solutions should have similar conductances: 0.1 M NaCl, 0.06 M CaCl₂, and 0.16 M sodium acetate.

The electrolyte identity and concentration must be carefully chosen for optimum, quantitative electrophoretic separation. The purpose of the electrophoresis electrolyte is to maintain a high-voltage gradient across the sample-containing solution in the capillary (this requires that the conductivity of the electrolyte be large compared to the conductivity of sample). Often the electrophoresis electrolyte also includes a buffer to control pH.

In order to obtain quantitative elemental speciation, interaction of the electrolyte with the sample must be avoided or at least carefully chosen. For example, if the electrolyte anion forms a complex with free analyte metal ions, the fraction of free ions versus metal–ligand complex originally present in the sample may be not be the same following electrophoretic separation.

When a high voltage is applied to a fused silica capillary, a static Stern layer, ~3–500 nm wide is formed.⁴⁵ Analyte ions can become trapped in this layer, thereby reducing sensitivity. The loss generally becomes worse when the applied voltage is increased, the electrolyte cation charge is smaller, the charge on the analyte ion is larger, or the concentration of the analyte ion is smaller (Table 1). A highly charged cation is best to minimize the loss of sensitivity due to the trapping of analyte ions in a static layer in the capillary. If the electrolyte cation has a large charge, it successfully competes with analyte ions for negatively charged sites within the Stern layer so that little analyte is lost. If the electrolyte cation has a smaller positive charge than the analyte ions, then a significant fraction of the analyte ions can be trapped in the Stern layer.⁵² There was less than a 10% loss of signal from Co²⁺ or Li⁺ analytes when CaCl₂ was used as the electrophoresis electrolyte with an applied voltage of 4 kV. In contrast, loss of signal from Co²⁺ analyte (present at 0.2 ppm in the injected sample) was almost 80% when a NaCl electrolyte was used with an applied voltage of 10 kV. It is not clear why the loss of signal due to Li⁺ analyte is not less severe when the CaCl₂ electrolyte was used in place of NaCl for an applied voltage of 10 kV.

(52) Roberts, G. O.; Rhodes, P. H.; Snyder, R. S. *J. Chromatogr.* **1989**, *480*, 35–67.

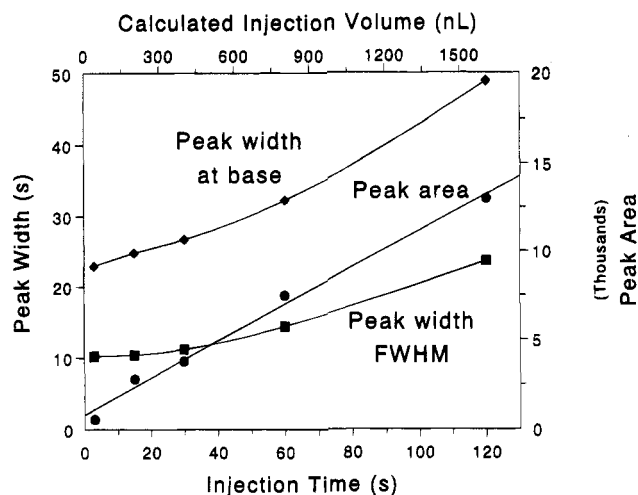


Figure 6. Effect of injection time on peak width (at base and fwhm) and peak area: Cr₂O₇²⁻, 0.06 M sodium acetate electrolyte, pH was ~8.2, and 10 kV applied voltage.

Effect of Injection Volume on Peak Width and Peak Area.

The total volume of the capillary was 4.3 μ L. The injection volume should be less than 10% of the capillary volume.⁴⁰ The injection volume, V , can be estimated from the following equation:⁴⁵

$$V = \left(\frac{\rho g r^2 \Delta h t_i}{8 \eta L} \right) (\pi r^2)$$

where ρ is the density of the sample, g is the gravity constant, Δh is the height of the reservoir relative to the outlet end of the capillary, r is the radius of the capillary, t_i is the injection time, η is the sample viscosity, and L is the capillary length.

Using the above equation, an injection volume of ~200 nL is calculated for the hydrostatic injection procedure used in these studies. In order to determine the injection volume experimentally, two measurements were made. In one measurement, Sr was added to the electrophoresis electrolyte at a concentration of 1 ppm and sample was continuously introduced into the plasma at a rate of 2 μ L/min, with no voltage applied. Knowing the volume of the capillary and the liquid flow rate, the total signal due to one capillary volume of sample was determined. The second measurement was the peak area due to injection of a 1 ppm Sr sample into the electrophoresis capillary (with no Sr in the electrophoresis electrolyte). The ratio of the two measurements is equal to the ratio of the capillary volume to the injection volume. The experimentally determined injection volumes were approximately 140 nL for the 50 cm long capillary and 80 nL for the 40 cm long capillary.

The effect of injection time on peak width (at base and the full width at half-maximum (fwhm)) and peak area, both calculated using the PeakFit software with an exponentially modified Gaussian peak shape, is shown in Figure 6. When the injection time was increased from 3 to 30 s, the peak area increased by a factor of ~7, but the peak width only increased by 17%. The calculated injection volume (using the above equation) for an injection time of 3 s is 40 nL. For an injection time of 30 s, the injection volume is 400 nL. An injection time of 15 s was chosen to maximize peak area while minimizing degradation of peak width and, therefore, resolution.

Effect of Nebulizer Gas Flow Rate. The nebulizer gas flow rate affects the forced liquid flow through the capillary, aerosol

Table 2. Effect of Nebulizer Gas Flow Rate on Cr₂O₇²⁻ Peak Characteristics^a

nebulizer gas flow rate (L/min)	elution time (s)	peak width (s)	fwhm (s)	peak area (counts)	no. of theor plates
0.67	180	58	22	2200	350
0.90	89	20.1	10.6	2700	600
1.26	73	18	5	354	1170

^a Detection by ICP-OES. Electrolyte was 0.04 M NaCl. The applied voltage was 10 kV.

formation and transport processes (including what fraction of aerosol reaches the plasma), spray chamber clearout time, and optimum location in the ICP for signal acquisition. Therefore, the optimum nebulizer gas flow rate will depend on a combination of its effect on electrophoretic resolution, elution time, and signal magnitude.

Table 2 shows the effect of nebulizer gas flow rate on Cr₂O₇²⁻ elution time, peak width, full width at half-maximum, peak area (signal magnitude), and number of theoretical plates. The elution times become shorter, peak widths narrower, and number of theoretical plates larger as the gas flow rate is increased. The elution times are shorter because the forced liquid flow rate through the capillary increased. The peak widths become narrower because either longitudinal diffusion is reduced (due to the smaller time the analyte spends in the capillary) or there is a faster washout time of the spray chamber. The calculation of the number of theoretical plates must be interpreted with some caution because a Gaussian peak shape is assumed while the experimental peak shapes are not Gaussian. However, the data show that the increase in the forced liquid flow rate did not result in a loss of separation efficiency.

There is an optimum nebulizer gas flow rate for maximum sensitivity. If the nebulizer gas flow rate is too low, the efficiency of generation of a fine aerosol and transport of the aerosol through the spray chamber and into the ICP will be low. If the nebulizer gas flow rate is too high, the amount of signal produced in the analytical region of the plasma per atom or ion in the ICP will be reduced, due to cooling of the plasma by the cold gas and liquid aerosol. Therefore, the nebulizer gas flow rate was optimized to maximize sensitivity.

Assessment of Analyte Transport, Signal Generation, and Sensitivity. In order to roughly assess the analyte transport efficiency, ⁸⁸Sr⁺ ICP-MS signals obtained using a standard cross-flow nebulizer and Scott-type spray chamber with a sample uptake rate of 1.0 mL/min were compared to signals produced using the CE interface system (Table 3). Signals produced from 1 ppm Sr were a factor of 40 times smaller when sample was continuously introduced into the capillary in a concentric nebulizer (with an open spray chamber) at a flow rate of 2 μ L/min rather than using the standard nebulizer and spray chamber with a 500 times larger sample uptake rate.

The signal per mass of analyte delivered to the nebulizer per unit time is a factor of ~ 12 larger for the capillary in a concentric nebulizer with open spray chamber than the standard cross-flow nebulizer and Scott-type spray chamber. This is likely due to two factors. First, the primary aerosol size generally decreases as the

Table 3. Comparison of Relative ⁸⁸Sr⁺ ICP-MS Signal and Relative Signal per Microliter per Minute of Sample Consumed^a

spray chamber	sample delivery (μ L/min)	nebulizer	rel signal	rel signal (per μ L/min) sample to nebulizer
Scott	1000 ^b	PE cross flow	61.9 ^c	0.12 ^c
open	2	capillary in concentric	1.5 ^c	1.5 ^c
open	2 ^d	capillary in concentric	1.0 ^e	1.0 ^e

^a Sample was 1 ppm Sr. ^b Typical ICP-MS sample introduction system for total elemental analysis. ^c Sample introduced continuously, average signal. ^d 0.14 μ L injected. ^e Signal peak height.

nebulizer gas to sample liquid ratio increases.⁵³⁻⁵⁸ Furthermore, the aerosol number density in the spray chamber decreases as the sample uptake rate decreases. As a result, analyte transport efficiencies generally increase as the sample uptake rate is decreased⁵⁸ so that a larger fraction of the aerosol produced by the nebulizer enters the plasma. Second, the use of an open rather than double-pass spray chamber will increase analyte transport efficiency.

If the analyte transport efficiency was $\sim 1.5\%$ for the cross-flow nebulizer and Scott-type spray chamber, the signals observed when the capillary in a nebulizer interface was used are consistent with a transport efficiency of $\sim 18\%$ (assuming that sensitivity in terms of signal per analyte atom that enters the plasma remains constant). When a 0.14 μ L sample was injected into the capillary, with no voltage applied, the signal peak height was a factor of 60 times smaller than the signal when sample was continuously introduced at a rate of 1.0 mL/min into a standard nebulizer with Scott spray chamber. The relative peak height of the CE signal (compared to an injection without voltage) will depend on the extent of focusing or sample stacking. The factor of 60 decrease in signal magnitude should be a lower limit on the CE signals compared to signals when sample is continuously introduced at a rate of 1.0 mL/min by using a nebulizer and double-pass spray chamber.

Calibration. Calibration curves for ICP-OES and ICP-MS are typically linear over 4-7 orders of magnitude. Figure 7 shows a CE/ICP-OES calibration curve (constructed from transient signals produced by eluting CE zones) for Sr²⁺ over 4 orders of magnitude. The slope of the log-log plot is 0.92. The least concentrated sample in the calibration curve shown in Figure 7 had a concentration 250 times the detection limit. The highest practical analyte concentration is more likely to be limited by loss of electrophoretic resolution than ICP quantitation linearity.

The CE/ICP-OES or CE/ICP-MS Cr sensitivity should be the same for Cr(III) and Cr(VI) because Cr-containing species are

- (53) Bates, L. C. Sample Aerosol Characterization and Study of Its Effect on Inductively Coupled Plasma Atomic Emission Spectrometry. Ph.D. Thesis, University of North Carolina-Chapel Hill, Chapel Hill, NC, 1991.
- (54) Canals, A.; Wagner, J.; Browner, R. F.; Hernandis, V. *Spectrochim. Acta* **1988**, *43B*, 1321-1335.
- (55) Sharp, B. L. *J. Anal. At. Spectrom.* **1988**, *3*, 613-652.
- (56) Canals, A.; Hernandis, V.; Browner, R. F. *Spectrochim. Acta* **1990**, *45B*, 591-601.
- (57) Canals, A.; Hernandis, V.; Browner, R. F. *J. Anal. At. Spectrom.* **1990**, *5*, 61-66.
- (58) Olesik, J. W.; Bates, L. C. Characterization of aerosols produced by pneumatic nebulizers for inductively coupled plasma sample introduction: effect of liquid and gas flow rates on volume based drop size distributions., submitted for publication in *Spectrochim. Acta*.

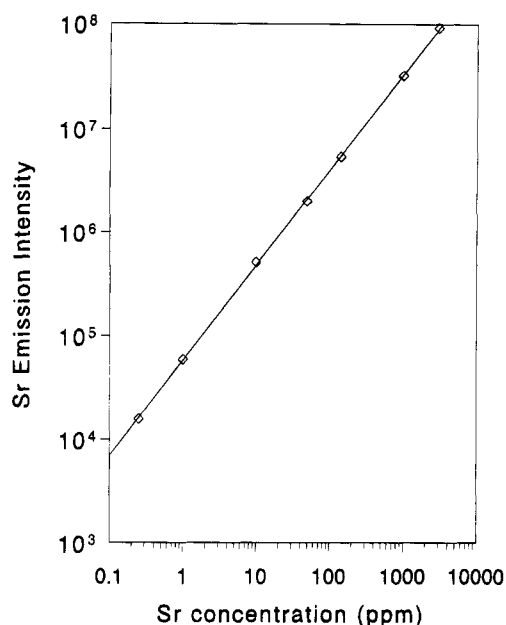


Figure 7. CE/ICP-OES calibration curve for Sr^{2+} : electrolyte was 0.06 M calcium chloride, pH was ~ 7 , and applied voltage was 4 kV.

efficiently converted into Cr^+ in the ICP. Calibration curves for Cr(III) and Cr(VI) , using ICP-OES detection, had slopes of 1.07 and 1.00, respectively, when displayed as log-log plots. The 95% confidence intervals for the slopes of calibration curves on linear scales for Cr(III) and Cr(VI) were 478.9–490.2 and 414.8–428.9 arbitrary emission intensity units per ppm Cr, respectively.

Initial Detection Limit Results. Liquid flow rates typically used for ICP spectrometry are ~ 1 mL/min. Capillary electrophoresis liquid flow rates are generally $2 \mu\text{L}/\text{min}$ or less. Detection limits for ICP-OES and ICP-MS are in the range of 0.1–100 ppb and 0.0001–1 ppb, respectively, for most elements. However, less than 2% of the sample aerosol generally reaches the plasma. Therefore, in terms of the amount of analyte entering the plasma per second, detection limits for ICP-OES are in the range of 0.034–34 pg/s. Detection limits for ICP-MS correspond to 0.034–340 fg/s entering the ICP. If sample could be transported into the plasma with high efficiency, and the responsivity (signal per picogram of sample entering the plasma per minute) remained constant, absolute detection limits in the picogram per second and femtogram per second range for CE/ICP-OES and CE/ICP-MS, respectively, should be possible for many elements.

Detection limits based on peak height and peak area are listed in Table 4. Detection limits will be partially dependent on the total measurement time for each analyte. Peak height based detection limits were calculated from the peak height and three times the standard deviation of at least eight background (off electrophoretic peak) points. Peak area based detection limits were calculated by adding data points across the peak. Five to eight sets of points (equal in number to the points across the peak) along the baseline were added. The standard deviation of the sets of added baseline points was calculated. The detection limit was calculated from the sensitivity divided by three times the standard deviation of the baseline points.

Peak area based detection limits were a factor of 5–30 better than the peak height based detection limits. The signal to noise ratio generally improves as the signal integration time is increased from 0.2 to 10 s.

Table 4. CE-ICP Spectrometry Detection Limits ($S/N = 3$) Obtained for CE/ICP-OES and CE/ICP-MS^a

detection	element	based on peak height			based on peak area		
		conc (ppb)	conc (M)	injected (pg)	conc (ppb)	conc (M)	injected (pg)
ICP-OES	Sr	9	1×10^{-7}	1	0.3	3×10^{-9}	0.04
	Cr	51	1×10^{-6}	7	6	1×10^{-7}	0.8
ICP-MS	Sr	1	1×10^{-8}	0.2	0.06	7×10^{-10}	0.008
	Cr	9	2×10^{-7}	1	2	4×10^{-8}	0.3
	As	8	1×10^{-7}	1	1	1×10^{-8}	0.1
	Sn	3	3×10^{-8}	0.4	0.5	4×10^{-9}	0.07
	Co	1	2×10^{-8}	0.1	0.09	2×10^{-9}	0.007
	Li	2	3×10^{-7}	0.2	0.06	9×10^{-9}	0.005

^a Applied voltage was 4 kV. In all cases, ICP-MS data were acquired from six different masses by peak hopping as described in the Experimental Section. Injection volume was $0.14 \mu\text{L}$ for all except Co and Li, where a $0.08 \mu\text{L}$ injection volume was used.

Peak area based detection limits for Sr and Cr CE/ICP-OES were within a factor of 10 of the detection limits observed using continuous sample introduction at a sample uptake rate of 1.0 mL/min. The detection limit for Sr using CE/ICP-OES with an injection volume of $0.14 \mu\text{L}/\text{min}$ and a 0.4 M calcium chloride electrophoresis electrolyte was 0.3 ppb, compared to 0.03 ppb for ICP-OES with a conventional sample introduction system at a sample uptake rate of 1.0 mL/min on the same instrument. Boumans⁵⁹ reported a detection limit of 0.3 ppb for conventional sample introduction at 1.0 mL/min by ICP-OES. The CE/ICP-OES detection limit for Cr (as Cr(III) or Cr(IV)) was ~ 6 ppb compared to 3 ppb using the same instrument with a conventional sample introduction system and a sample uptake rate of 1.0 mL/min. Considering that 500 times less sample is introduced to the nebulizer per unit time using the CE system compared to standard sample introduction systems for ICP-OES, the relatively small difference in detection limits is impressive. The higher responsivity is likely due to two factors. The analyte transport efficiency is likely near 20% for the CE nebulizer system rather than 1–2%, as discussed above. Second, the amount of light produced per ion in the plasma is likely higher because of less cooling due to fewer large aerosol droplets and a smaller total aerosol transport rate when the CE nebulizer system is used.^{60,61}

Detection limits for Sr, Cr, As, and Sn by CE/ICP-MS were roughly estimated from the data shown in Figure 3. Detection limits using ICP-MS with a conventional sample introduction system and a 1.0 mL/min sample uptake rate are less than 0.001 ppb for Sr and Co, 0.001–0.01 ppb for As and Sn, and 0.01–0.1 ppb for Cr and Li. So, the detection limits for CE/ICP-MS were a factor of 6–200 times worse than ICP-MS detection limits using standard nebulizers and spray chambers with a sample uptake rate of 1.0 mL/min. Plasma power, sampling depth, and ion optics settings were not optimized for the CE sample introduction system, so further improvements are possible. However, the detection limit obtained for Sr (0.06 ppb) corresponds to 8 fg (90 amol, 54 million atoms) of Sr in the $0.14 \mu\text{L}$ injection volume.

(59) Boumans, P. W. J. M. *Line Coincidence Tables for Inductively Coupled Plasma Atomic Emission Spectrometry*, 2nd ed.; Pergamon Press: Oxford, U.K., 1984.

(60) Olesik, J. W.; Den, S.-J. *Spectrochim. Acta* 1990, 45B, 731–752.

(61) Olesik, J. W.; Kinzer, J. A.; Harkleroad, B. *Anal. Chem.* 1994, 66, 2022–2030.

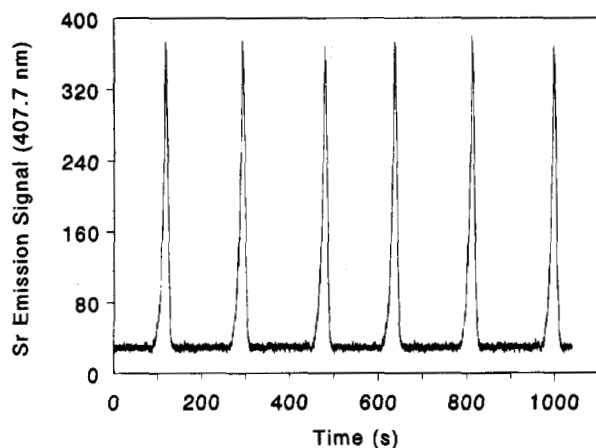


Figure 8. Repeated injections of Sr^{2+} (0.06 M calcium chloride electrolyte, pH was ~ 8) showing reproducibility of peak heights and shapes.

About 20 elements have ICP-MS detection limits⁶² similar to Sr, so CE/ICP-MS, even without further optimization, should provide detection limits that are adequate for a variety of practical applications including many environmental samples. Another 30 elements have ICP-MS detection limits that are a factor of ~ 10 worse than Sr.⁶²

Detection limits could be improved by a factor of 10–200 by use of electromigration sample injection.^{44,63} However, electromigration sample injection has some disadvantages including the following: only negative or positive ions could be injected at one time unless the electroosmotic flow is large enough to overcome the migration of ions away from the capillary and the injection would be dependent on the mobility of the analyte ions in the sample.

Reproducibility. Figure 8 shows the reproducibility in peak height and shape for six successive injections. The relative standard deviation of the peak height and peak area measurements were 1.3% and 2.3%, respectively.

In order to test the reproducibility of the system, a series of measurements were made and the interface was dismantled (the capillary was removed from the nebulizer) and then reinserted several hours later. A second series of measurements were made. The relative standard deviations of the entire set of measurements were 3.3% and 8.7% for the peak width and peak area, respectively. Reproducibility in elution times were typically 1–3% relative standard deviation.

Potential Sample Types Amenable To Analysis by CE-ICP Spectrometry. Figures 2, 3, and 5 demonstrated that ions with different charge states in solution can be separated and detected by CE-ICP. Neutral organometallic species, such as ferrocene, can also be separated from free ions.⁶⁴

It is also possible to separate free ions from metal–ligand complexes, as shown in Figure 9. Three different samples were used: one contained only Cu^{2+} , one had an excess of EDTA so that all Cu was present as CuEDTA^{2-} , and the third contained a mixture of Cu^{2+} and CuEDTA^{2-} . Free Cu^{2+} ions were separated from CuEDTA^{2-} ions. The experimental ratio of Cu^{2+} to CuEDTA^{2-}

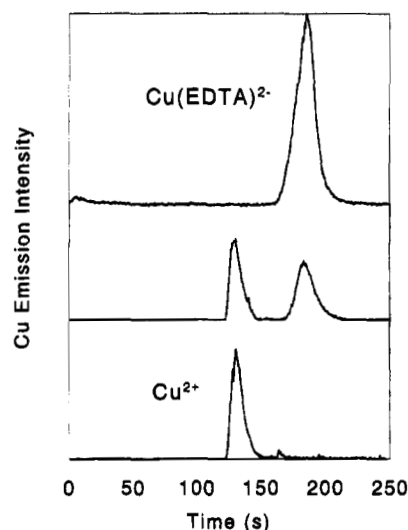


Figure 9. CE/ICP-OES electropherogram for samples containing Cu^{2+} , CuEDTA^{2-} , and a mixture of Cu^{2+} and CuEDTA^{2-} : 0.06 M calcium chloride electrolyte, pH ~ 5 , and 4 kV applied voltage.

peak areas was within 10% of the ratio of Cu^{2+} to CuEDTA^{2-} concentrations predicted by the MINTEQA2 equilibrium model. In order to quantitatively separate free metal ions from the metal–ligand complex, the relative concentrations must not be changed by the separation process. Furthermore, the kinetics must be slow enough to prevent rapid interconversion of the metal ion and metal–ligand complex. The separation shown in Figure 9 is not surprising since CuEDTA^{2-} is a very stable metal–ligand complex. However, it does indicate that the exchange kinetics are slow enough on the time scale of the separation to obtain two separate peaks rather than one peak which depends on the weighted average of the mobilities of the two species.⁶⁵ Further investigation is necessary to determine whether a wide range of metal–ligand complexes are amenable to quantitative separation from free metal ions under a range of chemical conditions (pH, etc.).

In two experiments (results shown in Figures 10 and 11), a sample containing free metal ions was injected into the electrophoresis capillary which contained a complexing ligand. Two peaks are observed in the electropherogram when Sr^{2+} was injected into a capillary containing acetate as the electrolyte anion (Figure 10) (Na^+ was the electrolyte cation). The pH was 8.2. The ratio of peak areas (0.866–0.134, determined by PeakFit) is in excellent agreement with the MINTEQA2 equilibrium model prediction that 86.7% of the Sr should exist as Sr^{2+} and 13.3% should exist as $\text{Sr}(\text{CH}_3\text{COO})_2$ in a solution at equilibrium. The concentration of Sr^{2+} in the injected sample volume and the concentration of CH_3COO^- in the electrolyte were input into MINTEQA2.

Two main peaks and one small peak were observed when Fe^{3+} was injected into a NaCl electrophoretic electrolyte (Figure 11). According to equilibrium model calculations (based on the concentration of Fe^{3+} in the injected sample and the concentration of Cl^- in the electrolyte), 28.1% of iron should be present as Fe^{3+} , 11.2% should exist as FeCl^{2+} , and 61% should exist as FeCl_2^+ . The ratio of peak areas determined by PeakFit was 0.24 to 0.15 to 0.61, in good agreement with the MINTEQA2 model prediction, given some uncertainty in the pH of the electrolyte solution. It is

(62) Montaser, A.; Golightly, D. W. *Inductively Coupled Plasmas in Analytical Atomic Spectrometry*, 2nd ed.; VCH Publishers: New York, 1992.

(63) Chien R.-L.; Burgi, D. S. *Anal. Chem.* **1992**, *64*, 1046–1050.

(64) Kinzer, J. A. *Elemental Speciation Using Capillary Electrophoresis-Inductively Coupled Plasma Emission and Mass Spectrometries*. M.S. Thesis, The Ohio State University, Columbus, OH, 1994.

(65) Iki, N.; Hoshino, H.; Yotsuyanagi, T. *J. Chromatogr.* **1993**, *652*, 539–546.

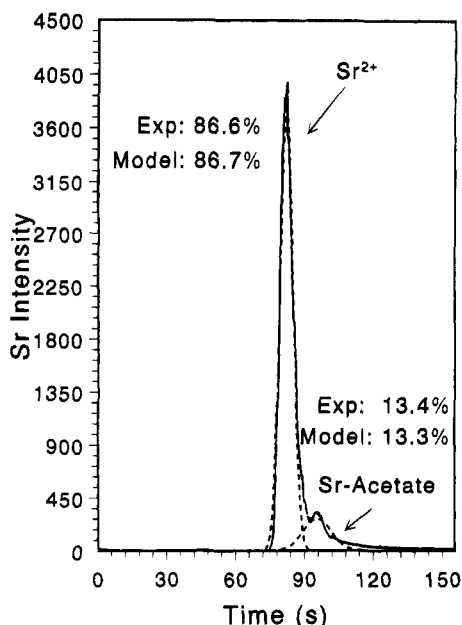


Figure 10. Electropherogram obtained when Sr^{2+} (100 $\mu\text{g/mL}$) was injected into 0.06 M sodium acetate. The pH was ~ 8.2 . A voltage of 10 kV was applied. The two peaks are consistent with Sr^{2+} and strontium acetate. Solid lines are experimental data; dashed lines are curve fit results.

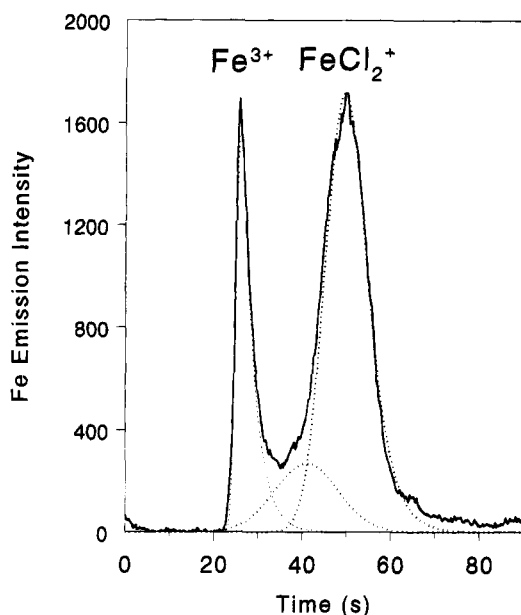


Figure 11. Electropherogram obtained when Fe^{3+} (1000 $\mu\text{g/mL}$) was injected into 0.04 M NaCl. The pH was ~ 7 . A voltage of 10 kV was applied. Solid lines are experimental data; dashed lines are curve fit results. The three peaks, in their elution order, estimated by the peak-fitting software were Fe^{3+} (24% of total area), FeCl_2^+ (15% of total area), and FeCl_2^+ (61% of total area).

somewhat surprising to obtain separate peaks for these species when the electrolyte contains the complexing ligand. However, if correct quantitative results can be obtained, as suggested by these results and those for the Sr^{2+} /strontium acetate system discussed above, it may be possible to measure metal–ligand stability constants in this manner.

The ability to measure stability constants for metal–ligand complexes in both aqueous and mixed aqueous/organic solvents is important for a number of applications including understanding of metal pollutant transport and remediation. Currently, titrations

or competitive lanthanide ion probe spectroscopy are used to measure stability constants of metal–ligand complexation.^{66,67} Titrations are time consuming and tedious, often lack sharp, easily detectable end points, and are difficult to carry out when the species of interest are present at low concentration. Competitive lanthanide ion probe spectroscopy is limited to simple samples and species with stability constants similar to those for the probe ion–ligand complexation.

CE-ICP spectroscopy may be amenable to rapidly, conveniently measure stability constants for a wide range of metal ions and ligands in complex as well as simple samples. By measuring the free metal ion concentration and the metal–ligand complex(es) concentration(s) using ICP spectrometry, the stability constant can be calculated if the pH and the $\text{p}K_a$ of the ligand are known. Further, if the ligand is present in high enough concentration, it will be possible to directly measure the free metal ion concentration, the metal–ligand complex(es) concentrations(s), and the free ligand concentration (by detecting C for organic ligands).

Recently, Erim et al.⁶⁸ described the use of capillary electrophoresis based measurements of stability constants of metal–ligand complexation direct UV detection of the free ligand and metal–ligand complex concentrations. They stated that, based on computer simulations, the method is limited to cases for complexation with neutral ligands. This is because the simulation predicts that the mobilities of the free metal ion and the metal–ligand complex must be the same so that they are not separated in the capillary. The examples above of metal ion complexation with EDTA, acetate, and chloride are cases where the ligands are charged, but the results suggest that this approach is quantitatively successful. It is also possible to measure stability constants by CE when the two components are not separated but the elution time of the peak is related to the weighted average of the mobilities of the free ion and ion–ligand complex.⁶⁹ Cleveland et al.⁷⁰ recently reported the use of capillary electrophoresis to determine $\text{p}K_a$ values of organic molecules at low solute concentrations, which cannot be performed by potentiometric titrations.

CONCLUSIONS

The initial results suggest that the combination of capillary electrophoresis and inductively coupled plasma optical emission or mass spectrometry holds great promise for rapid elemental speciation at concentrations as low as part per million to part per billion levels. Elemental ions with different charge states, metal–ligand complexes, and organometallic species can be separated and detected using CE-ICP spectrometry. There is evidence that it may be possible to use CE-ICP spectrometry to measure stability constants for metal–ligand complexation.

Detection limits for CE/ICP-OES, using a 0.14 μL sample injection and the capillary inserted into a nebulizer sample introduction system, were within a factor of 10 of those obtained using a conventional nebulizer/spray chamber and continuous sample uptake of 1.0 mL/min. Detection limits for CE/ICP-MS were more than a factor of 20 poorer than those obtained with

(66) Dobbs, J. C.; Susetyo, W.; Knight, F. E.; Castles, M. A.; Carreira, L. A. *Anal. Chem.* **1989**, *61*, 483.

(67) Dobbs, J. C.; Susetyo, W.; Carreira, L. A. *Anal. Chem.* **1989**, *61*, 1519.

(68) Erim, F. B.; Boelens, H. F. M.; Kraak, J. C. *Anal. Chim. Acta* **1994**, *294*, 155–163.

(69) Chu, Y.-H.; Avila, L. Z.; Biebuyck, H. A.; Whitesides, G. M. *J. Med. Chem.* **1992**, *35*, 2915–2917.

(70) Cleveland, J. A., Jr.; Benko, M. H.; Gluck, S. J.; Walbroehl, Y. M. *J. Chromatogr. A* **1993**, *652*, 301–308.

continuous sample introduction at a sample consumption rate of 1.0 mL/min. However, the CE/ICP-MS detection limits were in the 0.06–2 ppb range for the elements investigated. The 0.06 ppb Sr detection limit corresponded to 90 amol or 54 million molecules in the original injected sample. At least 20 other elements should have similar detection limits. The detection limits obtained in these initial studies are sufficient for many practical environmental, biological, geological, and medical applications.

While the initial results reported in this paper are promising, a number of questions must be more completely addressed. A wide variety of elements and species should be studied. Quantitation of multispecies systems must be further investigated. In particular, potential changes in the sample composition during the separation process must be evaluated for a wide range of sample types. The accuracy of species quantitation in practical environmental, medical, geological, and biological samples must be assessed. One of the difficulties in testing elemental speciation methods is the lack of suitable mixed-species standards. It may be necessary to use buffer systems to control the pH of the electrophoresis electrolyte. Experiments are now underway in our laboratories using a series of well-behaved multispecies systems that are amenable to accurate model prediction of the species concentrations. Samples with a range of pH values, metal–ligand complex stability, and conductivity are being investigated for both sample speciation and formation constant measurement by CE-ICP spectrometry. Extension of the CE-ICP spectrometry technique to mixed-solvent systems is also being pursued.

Further reduction of analysis times is being sought. Sources of in-capillary and postcapillary band broadening are being

assessed. Use of higher voltages to further improve separation efficiency is being explored. Modification of the interface to reduce the ratio of forced flow to electroosmotic flow, which should improve electrophoretic separation efficiency, is also being investigated.

ACKNOWLEDGMENT

Support for this research was provided by the U.S. Geological Survey Water Resources Program, the National Science Foundation (Grant CHE 9217170), and The Ohio State University. The ARL 34000 inductively coupled plasma optical emission spectrometer was donated by R. J. Reynolds Co. The Perkin Elmer Corp. is thanked for use of a Perkin Elmer Sciex ELAN 5000 inductively coupled plasma mass spectrometer on which some of the CE/ICP-MS data were acquired and for partial support for the instrument now in our laboratory. Dr. Lisa Lanning is acknowledged for providing the Cu^{2+} and $\text{Cu}(\text{EDTA})^{2-}$ CE/ICP-OES data. Portions of this work were presented at the XXth Federation of Analytical Chemistry and Spectroscopy Societies Meeting, Detroit, MI, October 1993, paper 659; the 1994 Winter Conference on Plasma Spectrochemistry, San Diego, CA, January 1994, paper 75, and the 1994 Pittsburgh Conference on Analytical Chemistry, Chicago, IL, March 1994, paper 1079.

Received for review September 19, 1994. Accepted October 24, 1994.*

AC940933B

* Abstract published in *Advance ACS Abstracts*, November 15, 1994.